

Vectorized implementation of primal hybrid FEM in MATLAB

Harish Nagula Mallesham¹, Kamana Porwal², Jan Valdman^{3,4},
Sanjib Kumar Acharya^{1*}

¹ Institute of Chemical Technology Mumbai , IndianOil Odisha Campus, Bhubaneswar, 751013, Odisha, India.

²Department of Mathematics, Indian Institute of Technology Delhi, New Delhi, 110016, Delhi, India.

³ Faculty of Information Technology, Czech Technical University in Prague, Thákurova 9, 16000 Prague, Czech Republic.

⁴The Czech Academy of Sciences, Institute of Information Theory and Automation, Pod vodárenskou věží 4, 18208, Prague 8, Czech Republic.

*Corresponding author(s). E-mail(s): sk.acharya@ioct.ictmumbai.edu.in;

Contributing authors: mat21h.nagula@stuiocb.ictmumbai.edu.in;

kamana@maths.iitd.ac.in; jan.valdman@utia.cas.cz ;

Abstract

We present efficient MATLAB implementations of the lowest-order primal hybrid finite element method (FEM) for linear second-order elliptic and parabolic problems with mixed boundary conditions in two spatial dimensions. We employ the Crank-Nicolson finite difference scheme for the complete discrete setup of the parabolic problem. All the codes presented are fully vectorized using matrix-wise array operations. Numerical experiments are conducted to show the performance of the software.

Keywords: finite elements, primal hybrid method, elliptic problem, parabolic problem, vectorization, MATLAB

MSC Classification: 35-04 , 65N30 , 65N06 , 35J25 , 35K20 , 35K57

1 Introduction

MATLAB is a popular computing platform in academia and industry, with many built-in functions and toolboxes developed by Mathworks Computer Software Corporation. However, codes containing for loops, particularly the assembly of finite elements of stiffness and mass matrices in MATLAB are extremely slow compared to C and FORTRAN (cf. [1, 2]). To overcome this issue, an efficient and flexible MATLAB assembly procedure of nodal element stiffness and mass matrices for 2D and 3D was introduced by Rahman and Valdman [3]. They vectorized for-loops by extending the element-wise array operations into matrix-wise array operations, where the array elements are matrices rather than scalars, resulting in a faster and more time-scalable algorithm. This idea is exploited for the MATLAB assembly of 2D and 3D edge elements by Anjam and Valdman in [4]. In [5], Funken et al. adopted a similar approach while assembling the element stiffness matrices. For more detailed literature, we refer to Cuvelier et al., see [6], Moskovka and Valdman [7] and the references therein.

In this paper, we present an efficient MATLAB implementation procedure of the primal hybrid finite element method, which is based on an extended variational principle introduced by Raviart and Thomas in [8] for elliptic problems. Acharya and Porwal [9, 10] extended this technique to parabolic second- and fourth-order problems and established the optimal order error estimates. The benefit of this method is that two unknown variables (primal and hybrid) can be computed simultaneously without losing accuracy. The constrained space using Lagrange multipliers leads to a non-conforming space; for instance, the lowest-order primal hybrid FEM (using unconstrained space) is equivalent to the Crouzeix-Raviart nonconforming (using constrained space) finite element space. It is also called the generalized nonconforming method. For a detailed review of the literature and applications, see [9–12] and the references therein. To the best of the author's knowledge, no work has been reported on the implementation procedure of this method.

The main contributions are as follows.

- Edge generation function `edge.m` (cf. [2]) and a uniform mesh refinement function based on red-refinement (cf. [13, 14]) have been vectorized using matrix-wise array operations.
- We present a vectorized implementation of the lowest-order primal hybrid FEM for a second-order general elliptic problem with mixed boundary conditions.
- Also, we implement this method for the general second-order parabolic problem with mixed boundary conditions using the Crank-Nicolson finite difference scheme in the temporal direction.
- Numerical experiments have been conducted, and run-time has been presented. The experiments were carried out using MATLAB R2020a on a computer equipped with an i5 – 10210U CPU operating at a frequency of 1.60GHz-2.10 GHz, with 16GB RAM and a x64-based processor with 1TB of system memory. A linear regression analysis shows that the codes have an approximate optimal-order time scale.
- The software can be downloaded through the following link: <https://www.mathworks.com/matlabcentral/fileexchange/136359>.

The outline of this paper is as follows: In Section 2, we present the required data structure to present the primal hybrid FEM and its implementation procedures. The primal

hybrid finite element algebraic formulation for the elliptic problem and its MATLAB implementation have been discussed in Section 3. Implementation of the primal hybrid FEM with the Crank-Nicolson scheme in the time direction for parabolic problems is presented in Section 4. We give our concluding remarks in Section 5.

2 Triangulation and geometric structure

Let $\Omega = (0, 1)^2$ be the computational domain with boundary $\Gamma = \bar{\Gamma}_D \cup \bar{\Gamma}_N$, where $\bar{\Gamma}_D$ and $\Gamma_N = \Gamma \setminus \bar{\Gamma}_D$ are the Dirichlet and Neumann boundary, respectively. We use the Sobolev spaces $H^m(\Omega)$, $H(\text{div}, \Omega)$ in the domain Ω , $m \in \mathbb{R}_{\pm}$ [15]. With the mesh parameter h , let \mathcal{T}_h be a regular family of triangulations of the set $\bar{\Omega}$ in the sense of Ciarlet [15] with shape regular triangles T whose diameters $h_T \leq h$ are such that $\bar{\Omega} = \bigcup_{T \in \mathcal{T}_h} \bar{T}$.

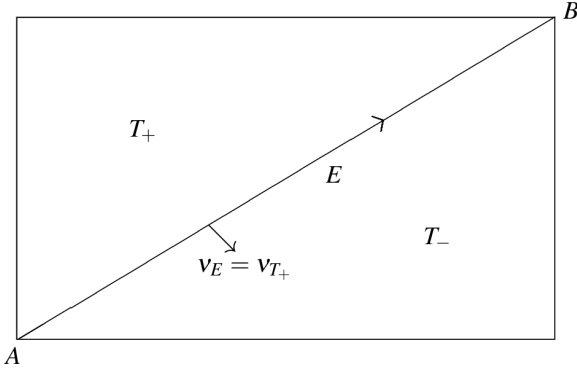


Fig. 1: A pair of adjacent triangles (T_+, T_-) with a common edge $E = \partial T_+ \cap \partial T_-$, initial node A , end node B and outward unit normal $\nu_E = \nu_{T_+}$.

For any triangle T , let ∂T denote the boundary of T and let ν_T be the outward unit normal to ∂T . Let

$$\mathcal{E}^h = \mathcal{E}_\Omega^h \cup \mathcal{E}_D^h \cup \mathcal{E}_N^h$$

be the set of all edges E of \mathcal{T}_h where \mathcal{E}_Ω^h denotes the set of all interior element edges,

$$\mathcal{E}_D^h = \{E \in \mathcal{E}^h : E \subset \bar{\Gamma}_D\}$$

denotes the set of edges on the Dirichlet boundary and

$$\mathcal{E}_N^h = \{E \in \mathcal{E}^h : E \subset \bar{\Gamma}_N\}$$

denotes the set of edges on the Neumann boundary. The following notations will be used throughout the article:

$$\begin{aligned}
\mathcal{N} &= \text{set of vertices of element } T \in \mathcal{T}_h, & nE &= \text{card}(\mathcal{T}_h), \\
m_E &= \text{mid-point of } E \in \mathcal{E}^h, & N &= 3 \times nE, \\
\mathcal{N}_m &= \text{set of mid-points } m_E \text{ of the edges } E \in \mathcal{E}^h, & L &= \text{card}(\mathcal{E}_\Omega^h \cup \mathcal{E}_D^h), \\
\mathcal{N}_m(\Gamma_D) &= \text{set of midpoints of the edges } E \in \mathcal{E}_D^h, & \text{nrEdges} &= \text{card}(\mathcal{E}^h), \\
\mathcal{N}_m(\Gamma_N) &= \text{set of midpoints of the edges } E \in \mathcal{E}_N^h, & N_D &= \text{card}(\mathcal{E}_D^h), \\
\text{card}(S) &= \text{cardinality of the set } S, & N_\Omega &= \text{card}(\mathcal{E}_\Omega^h), \\
\text{conv}\{A, B\} &= \text{Convex hull of } A \text{ and } B, & N_n &= \text{card}(\mathcal{E}_N^h).
\end{aligned}$$

The intersection of two distinct triangles of \mathcal{T}_h is either empty or non-empty. They share one complete edge $E = \text{conv}\{z_1, z_2\}$ or a node z_1 in the non-empty case. Fig. 1 depicts two adjacent triangles T_+ and T_- with a common edge $E = \text{conv}\{A, B\}$. Let $\mathcal{N} = \{z_1, \dots, z_{\text{card}(\mathcal{N})}\}$ be the set of vertices (nodes) z_l , $1 \leq l \leq \text{card}(\mathcal{N})$ with coordinates $(x_l, y_l) \in \mathbb{R}^2$. For an edge $E = \text{conv}\{z_i, z_j\}$ such that z_i and z_j are ordered counterclockwise, its outward unit normal defined as:

$$v_E = (y_j - y_i, x_j - x_i) / |E|,$$

where $|E|$ is the length of E . We define the jump of a scalar-valued function v on any $E \in \mathcal{E}^h$ such that $E = \partial T_+ \cap \partial T_-$ (T_+ and T_- are adjacent triangles in \mathcal{T}_h) as:

$$[[v]]_E = (v|_{T_+})|_E - (v|_{T_-})|_E$$

and for a boundary edge E such that $E = \partial T \cap \Gamma$, where $T \in \mathcal{T}_h$, we define $[[v]]_E = v|_T v_E$.

Let i, j, k represent the global numbering of nodes of a triangle $T = \text{conv}\{z_i, z_j, z_k\}$. Let E_i, E_j, E_k be edges of triangle T_+ and E_p, E_q, E_r be edges of triangle T_- for two adjacent triangular elements $T_+ = \text{conv}\{z_i, z_j, z_k\}$ and $T_- = \text{conv}\{z_p, z_q, z_r\}$ in \mathcal{T}_h as in Fig. 2.

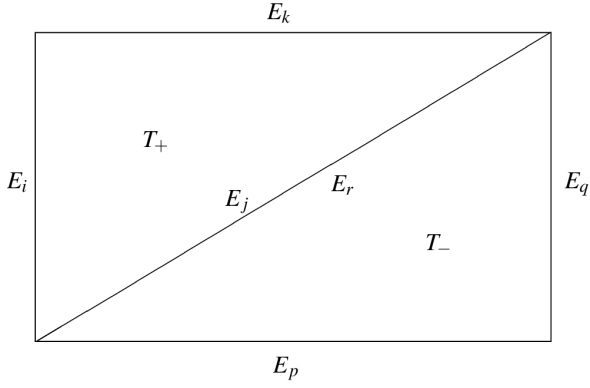


Fig. 2: Depiction of a general numbering of edges in a mesh with two adjacent triangles.

For a triangular element, $T = \text{conv}\{P_1, P_2, P_3\}$, where

$$P_1 = (x_1, y_1), \quad P_2 = (x_2, y_2), \quad P_3 = (x_3, y_3)$$

are vertices of T , opposite edges are

$$E_1 = \text{conv}\{P_2, P_3\}, \quad E_2 = \text{conv}\{P_1, P_3\}, \quad E_3 = \text{conv}\{P_1, P_2\},$$

mid-point of edges are

$$mE_1 = (P_2 + P_3)/2, \quad mE_2 = (P_1 + P_3)/2, \quad mE_3 = (P_1 + P_2)/2,$$

and area of the element is denoted as $|T|$.

2.1 Data representation of the triangulation

We present the data structure of the initial triangulation of Ω with triangles in Table 1 and Fig. 3. The nodes and elements are stored in the rows of "coordinates.dat" and "elements.dat", respectively. The information about the boundary edges in \mathcal{E}_D^h and \mathcal{E}_N^h are stored in "Dirichlet.dat" and "Neumann.dat", respectively.

Table 1 coordinates.dat, elements.dat, Neumann.dat (consists of 2 boundary edges which are plotted in red) and Dirichlet.dat (remaining 2 boundary edges) data for the triangulation displayed in Fig. 3.

coordinates.dat		elements.dat			Dirichlet.dat		Neumann.dat	
0	0		5	1	2			
1	0		5	3	1			
0	1		5	4	3			
1	1		5	2	4			
0.5	0.5							

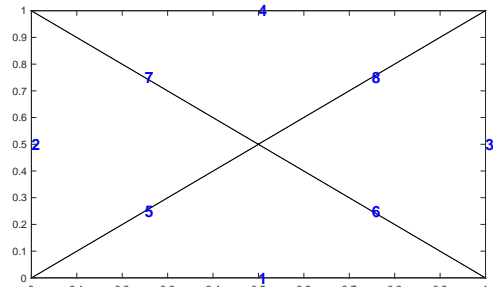
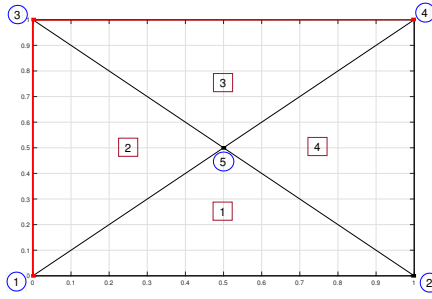


Fig. 3: Depiction of initial (level 0) triangulation (left) and the corresponding edges generated (right).

2.2 Vectorization of `edge.m`

In this subsection, we present a modified version of the function `edge.m` (whose inputs are `elements` and `coordinates` and outputs are `nodes2element(n2el)`, `nodes2edge(n2ed)` and `edge2element(ed2el)` (cf. Bahriawati and Carstensen, [2]). The following example intuitively explains the meaning of output matrices.

Example 1. Given the triangulation of Fig. 3, we have the following full versions of sparse matrices

$$\text{nodes2element} = \begin{pmatrix} 0 & 1 & 0 & 0 & 2 \\ 0 & 0 & 0 & 4 & 1 \\ 2 & 0 & 0 & 0 & 3 \\ 0 & 0 & 3 & 0 & 4 \\ 1 & 4 & 2 & 3 & 0 \end{pmatrix}, \quad \text{nodes2edge} = \begin{pmatrix} 0 & 1 & 2 & 0 & 5 \\ 1 & 0 & 0 & 3 & 6 \\ 2 & 0 & 0 & 4 & 7 \\ 0 & 3 & 4 & 0 & 8 \\ 5 & 6 & 7 & 8 & 0 \end{pmatrix}. \quad (2.1)$$

The 1st row of `nodes2element` tells us that the directed edge $1 \rightarrow 2$ belongs to the element 1 and the directed edge $1 \rightarrow 5$ belongs to the element 2. Note the directed edge $3 \rightarrow 1$ is stored in the 3rd raw and belongs to the element 2.

The matrix `nodes2edge` provides actual numbers of edges. The first raw reveals that the undirected edge $1 \leftrightarrow 2$ has number 1, the undirected edge $1 \leftrightarrow 3$ has number 2, and the undirected edge $1 \leftrightarrow 5$ has number 5.

Finally, the matrix `edge2element` contains nodes belonging to edges (the first two columns) and the connection of edges to elements (the remaining two columns).

$$\text{edge2element} = \begin{pmatrix} 1 & 2 & 1 & 0 \\ 3 & 1 & 2 & 0 \\ 2 & 4 & 4 & 0 \\ 4 & 3 & 3 & 0 \\ 5 & 1 & 1 & 2 \\ 2 & 5 & 1 & 4 \\ 5 & 3 & 2 & 3 \\ 5 & 4 & 3 & 4 \end{pmatrix}. \quad (2.2)$$

The fifth row tells us that the edge $5 \leftrightarrow 1$ belongs to the elements 1, 2. Clearly, the rows of `edge2element` with the fourth column entry equal to zero describe boundary edges that belong to one element only.

By removing for-loops of `edge.m` function, we provide a modified function:

```
[nodes2element, nodes2edge, edge2element]=edge_vec(elements, coordinates)
```

in which the interior edges (`intE`), exterior edges (`extE`), local edge numbering data for T_+ elements (`led`), and local edge numbering data for T_- elements (`ledTN`) can additionally be output.

2.2.1 nodes2element

The `nodes2element` function describes an element's global number as a function of its two vertices, with dimension $\text{card}(\mathcal{N}) \times \text{card}(\mathcal{N})$ defined as,

$$\text{nodes2element}(k, l) = \begin{cases} j & \text{if } (k, l) \text{ are numbers of the nodes of element number } j; \\ 0 & \text{otherwise.} \end{cases} \quad (2.3)$$

For the matrix `nodes2element`, the vectorized computation in MATLAB is as follows:

```

1 nE=size(elements,1); %number of elements
2 nC=size(coordinates,1); % number of nodes
3 I=elements(:,1);
4 J=reshape(elements(:,[2 3 1]), numel(elements), 1);
5 S=reshape([1:nE;1:nE;1:nE]', numel(elements), 1);
6 nodes2element=sparse(I, J, S, nC, nC);

```

Listing 1: Vectorization of the `nodes2element` matrix.

Here `nodes2element` is a sparse matrix from the triplets `I`, `J`, and `S` such that, $\text{nodes2element}(I(k), J(k)) = S(k)$, where `I`, `J` and `S` are column-vectors as shown in Fig. 4.

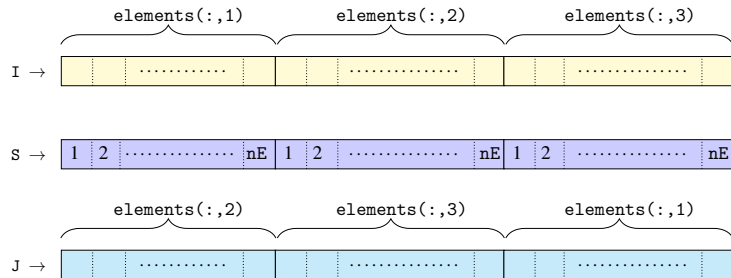


Fig. 4: Geometrical representation of `I`, `J`, and `S` vectors in MATLAB.

2.2.2 nodes2edge

The sparse matrix `node2edge` describes the global number of edges, with dimension $\text{card}(\mathcal{N}) \times \text{card}(\mathcal{N})$ defined as,

$$\text{nodes2edge}(k, l) = \begin{cases} j & \text{if } j - \text{th edge is connected between the} \\ & \text{two nodes with global numbering } (k, l); \\ 0 & \text{otherwise.} \end{cases} \quad (2.4)$$

The MATLAB code for the calculation of the matrix `nodes2edge` is as follows:

```

1 B=nodes2element+nodes2element';
2 [i,j]=find( triu(B));
3 nodes2edge=sparse(i,j,1:size(i,1),nC,nC);
4 nodes2edge=nodes2edge+nodes2edge';

```

Listing 2: Vectorization of the `nodes2edge` matrix.

In the above code, the variables i and j represent the row and column indices for the nonzero entries of the upper triangular part of the matrix B . The number of edges is denoted by $\text{nrEdges}=\text{size}(i,1)$.

2.2.3 edge2element

The row number $p1$ of the matrix `edge2element` represents the edge's initial node k and end node l , as well as the numbers m, n of elements T_+, T_- that share the edge, and the matrix `edge2element` has a dimension of $\text{nrEdges} \times 4$.

`edge2element (p1,[1,2]) = [k l] (k,l) are initial node and end node of edge p1.`

The Fig. 1 convention is used to specify the neighbor elements T_+, T_- with indices m and n . The entry of the matrix `edge2element(p1,3)` defines the element T_+ , which also specifies the orientation of the unit normal $\nu_E = \nu_{T_+}$ of the edge $E = T_+ \cap T_-$. If the edge $E \in \mathcal{E}_D^h \cup \mathcal{E}_N^h$, then the fourth entry `edge2element(p1,4)` is zero, indicating that ν_E lies on $\partial\Omega$.

$$\text{edge2element (p1,[3,4])} = \begin{cases} [m \ n] & \text{if the common edge } p1 \text{ belongs to element } m \text{ and } n; \\ [m \ 0] & \text{if the boundary edge } p1 \text{ belongs to element } m. \end{cases} \quad (2.5)$$

The MATLAB code for the vectorized calculation of the matrix `edge2element` is as follows:

```

1 %% to generate an element of edge
2 Inode=elements'; Inode=Inode(:,1); % initial nodes
3 Enode=elements(:,[2,3,1])'; Enode=Enode(:,1); % end nodes
4 Q=[Inode, Enode, nodes2element(sub2ind([nC nC],Inode,Enode)),nodes2element(sub2ind
    ([nC nC],Enode,Inode))];
5 p2 = nodes2edge(sub2ind([nC nC],Inode,Enode));
6 [uniquep2,uniqueIdx] = unique(p2); % find the indices of the unique p2
7 r=setdiff(1:numel(p2),uniqueIdx)'; % find the indices of the repeated values p2 or
    % find the repeated edges row indices of Q
8 Q(r,:)=[]; % removing the repeated edges in Q
9 edge2element(uniquep2,:)=Q;
10 %% To produce the interior edges
11 intE=find(edge2element(:,4));
12 %% To produce the exterior edges
13 extE=find(edge2element(:,4)==0);
14 %% To produce local edge number
15 localE=repmat([3;1;2],nE,1);
16 ledTN(p2,1)=localE; % local edge numbering to T- elements
17 localE(r)=[]; % removing the repeated local edges
18 led(uniquep2,1)=localE; % local edge numbering to T+ elements

```

Listing 3: Vectorization of the `edge2element` matrix.

In the above code

- Line 2-3: The column vectors, `Inode` and `Enode`, specify the initial and end nodes of every edge $E \in \mathcal{E}^h$ through their respective indices.
- Line 4: The vector `Q` concatenates the `Inode`, `Enode`, T_+ , and T_- , potentially resulting in the repetition of edges.
- Line 5: `p2` is a column vector containing the global edge number according to $\text{conv}\{ \text{Inode}, \text{Enode} \}$.
- Line 6-9: We assemble the `edge2element` with `Q` by removing the repetition of edges.
- Line 15: The local edge numbering of element T is $\{E_3, E_1, E_2\}$, that is $[3;1;2]$ in MATLAB.

- Line 16: With the help of repeated edges, we calculate the local edge numbering for T_- elements in `ledTN`.
- Line 18: With the help of unique edges, we compute the local edge numbering for T_+ elements in `led`.

2.3 Vectorization of `redrefine.m`

The function `redrefine_vec.m` performs uniform refinement of the computational domain.

```

1 function [coordinates,elements,Dirichlet,Neumann]=redrefine_vec(coordinates,
2 elements,n2ed,ed2el,Dirichlet,Neumann)
3 nE=size(elements,1); % number of elements
4 nrEdges=size(ed2el,1); % number of edges
5 %% Coordinates
6 Inode=ed2el(:,1); Enode=ed2el(:,2); % initial and end nodes of edge
7 c1=coordinates(Inode,:); c2=coordinates(Enode,:); % their coordinates
8 NCoord=(c1+c2)/2; % coordinates of new nodes or mid-point of edges
9 Marker=(size(coordinates,1)+1:size(coordinates,1)+nrEdges);
10 coordinates(Marker,:)=[NCoord(:,1) NCoord(:,2)];
11 %% Elements
12 CT=elements; % current triangle
13 CE= diag(n2ed(elements(:,[2 3 1]),elements(:,[3 1 2])));
14 M1=Marker(CE(1:nE)); M2=Marker(CE(nE+1:2*nE)); M3=Marker(CE(2*nE+1:3*nE));
15 elements((1:nE),:)=[M1' M2' M3'];
16 elements((nE+1:3:4*nE-2),:)=[CT(:,1) M3' M2'];
17 elements((nE+2:3:4*nE-1),:)=[CT(:,2) M1' M3'];
18 elements((nE+3:3:4*nE),:)=[CT(:,3) M2' M1'];
19 %% Dirichlet and Neumann boundary
20 if (~isempty(Dirichlet)), Dirichlet=refineEdges(Dirichlet); end
21 if (~isempty(Neumann)), Neumann=refineEdges(Neumann); end
22 function ed2n=refineEdges(ed2n)
23 nEdges=size(ed2n,1); % number of edges
24 Base=diag(n2ed(ed2n(:,1),ed2n(:,2)));
25 P=[ed2n(:,1) Marker(Base(:))' ed2n(:,2)];
26 ed2n(1:nEdges,:)=[P(:,1) P(:,2)];
27 ed2n(nEdges+1:2*nEdges,:)=[P(:,2) P(:,3)];
28 end
29 end

```

Listing 4: Vectorization of `redrefine` function.

- Line 4-9: The index of all new nodes is stored in a vector called `Marker`. The new mid-point coordinates are added to `coordinates` data by using `Marker` and concatenation.
- Line 10-17: For all triangles in the original mesh, three new triangles are created by the mid-point of the edges. Mark the new nodal numbers in `M1`, `M2`, and `M3` vectors. The connectivity of all these new triangles is stored in the `elements` data.
- Line 18-27: If there are \mathcal{E}_D^h in the original mesh, collect the Dirichlet edge data in `Base`. A new node is created at the mid-point of the Dirichlet edge. Then for each Dirichlet edge, we find the corresponding new mid-point node using `Marker`. Update the `Dirichlet` data with these new nodes. For the Neumann boundary, the code does the same thing as for the Dirichlet boundary, but with the `Neumann` data.

2.4 Run-time of `edge_vec.m` and `redrefine_vec.m`

Table 2 presents the run-time of vectorized versions of the functions `edge.m` and `redrefine.m` in MATLAB, as we increase the level of refinement. Level 0 corresponds to the

initial triangulation of the domain (Fig. 3), which consists of four triangular elements. In contrast, level 1 is the first uniform refinement of level 0, resulting in 16 triangular elements. For any $n \in \mathbb{N}$, level n is the uniform refinement of level $n-1$, and it contains 4^{n+1} triangular elements.

Table 2 Run-times: Vectorized code of **edge.m** and **redrefine.m**.

Level	nE	run-time (in sec)	
		edge_vec.m	redrefine_vec.m
5	4096	0.006	0.0001
6	16384	0.023	0.0008
7	65536	0.082	0.003
8	262144	0.41	0.15
9	1048576	2.04	0.68
10	4194304	8.66	2.90

Remark 1. Run-times for non-vectorized codes are much higher compared to vectorized codes; for instance, the run-times of **edge.m** and **redrefine.m** are 17114.35 and 2861.10 seconds, respectively, at level 9.

3 Implementation of second order elliptic model problem

3.1 Problem formulation

Consider the general second-order elliptic problem

$$-\nabla \cdot (A \nabla u + up) + \delta u = f \text{ in } \Omega, \quad (3.1)$$

$$u = u_D \text{ on } \Gamma_D, \quad (3.2)$$

$$(A \nabla u + up) \cdot v = g \text{ on } \Gamma_N, \quad (3.3)$$

where A is a symmetric and positive definite matrix whose entries are constants, p is a constant vector and δ is a constant. Also, f , u_D , and g are assumed to be sufficiently smooth.

We consider the broken Sobolev space (cf. [8]), i.e., a space of functions that belong to Sobolev space $H^1(T)$ on each element T ,

$$X = \{v \in L^2(\Omega) : v|_T \in H^1(T), \forall T \in \mathcal{T}_h\} = \prod_{T \in \mathcal{T}_h} H^1(T).$$

The broken Sobolev space has the norm $\|v\|_X = \left(\sum_{T \in \mathcal{T}_h} \|\nabla v\|_{L^2(T)}^2 \right)^{\frac{1}{2}}$. We shall denote by $H^{1/2}(\Gamma)$ the space of traces $v|_\Gamma$ over Γ of the functions $v \in H^1(\Omega)$ and $H^{-1/2}(\Gamma)$ denotes the dual space of $H^{1/2}(\Gamma)$. The Lagrange multiplier space is defined as

$$M = \left\{ \chi \in \prod_{T \in \mathcal{T}_h} H^{-1/2}(\partial T / \Gamma_N) : \text{there exists } \mathbf{q} \in H(\text{div}, \Omega) \text{ such that, } \mathbf{q} \cdot v_T = \chi \text{ on } \partial T / \Gamma_N, \forall T \in \mathcal{T}_h \right\}.$$

The Lagrange multiplier space is provided with the norm

$$\|\chi\|_M = \sup_{v \in X} \frac{\sum_{E \in \mathcal{E}^h / \mathcal{E}_N^h} \langle \chi, v \rangle_E}{\|v\|_X},$$

where $\langle \cdot, \cdot \rangle_E$ denotes the duality paring between $H^{-1/2}(E)$ and $H^{1/2}(E)$.

Primal hybrid formulation of (3.1)-(3.3) is to seek a pair of solutions $(u, \kappa) \in X \times M$ such that

$$a(u, v) + b(v, \kappa) = (f, v) + \langle g, v \rangle_{\Gamma_N} \quad \forall v \in X, \quad (3.4)$$

$$b(u, \chi) = \langle u_D, \chi \rangle, \quad \forall \chi \in M, \quad (3.5)$$

where

$$\begin{aligned} a(u, v) &= \sum_{T \in \mathcal{T}_h} \int_T ((A \nabla u + u p) \cdot \nabla v + \delta u v) \, dx, \\ b(v, \chi) &= - \sum_{E \in \mathcal{E}^h / \mathcal{E}_N^h} \langle \chi, v \rangle_E, \\ \langle u_D, \chi \rangle &= - \sum_{E \in \mathcal{E}^h / \mathcal{E}_N^h} \langle \chi, u_D \rangle_E. \end{aligned}$$

Here, the Lagrange multiplier

$$\kappa = (A \nabla u + u p) \cdot v_T \quad \text{on } \partial T / \Gamma_N, \quad \forall T \in \mathcal{T}_h \quad (3.6)$$

is associated with the constraint $u \in \{v \in H^1(\Omega) : v = u_D \text{ on } \Gamma_D\}$.

3.2 Discrete problem and algebraic formulation

Let P_k be the space of polynomials of degree $\leq k$, for integer $k \geq 0$. We define the finite-dimensional spaces $X_h \subset X, M_h \subset M$ as

$$\begin{aligned} X_h &= \prod_{T \in \mathcal{T}_h} P_1(T), \\ M_h &= \left\{ \chi_h \in \prod_{E \in \mathcal{E}^h / \mathcal{E}_N^h} P_0(E) : \chi_h|_{\partial T_+} + \chi_h|_{\partial T_-} = 0 \text{ on } T_+ \cap T_-, \text{ for any adjacent pair } T_{\pm} \in \mathcal{T}_h \right\}. \end{aligned}$$

We seek a pair $(u_h, \kappa_h) \in X_h \times M_h$ such that for all pairs $(v_h, \chi_h) \in X_h \times M_h$

$$\begin{aligned} \sum_{T \in \mathcal{T}_h} \int_T ((A \nabla u_h + u_h p) \cdot \nabla v_h + \delta u_h v_h) \, dx - \sum_{E \in \mathcal{E}^h / \mathcal{E}_N^h} \int_E \kappa_h [[v_h]]_E \, d\gamma \\ = \sum_{T \in \mathcal{T}_h} \int_T f v_h \, dx + \int_{\Gamma_N} g v_h \, d\gamma, \quad (3.7) \end{aligned}$$

$$-\sum_{E \in \mathcal{E}^h / \mathcal{E}_N^h} \int_E \chi_h [[u_h]]_E \, d\gamma = -\sum_{E \in \mathcal{E}^h / \mathcal{E}_N^h} \int_E \chi_h u_{Dh} \, d\gamma. \quad (3.8)$$

Note that the problem (3.7)-(3.8) has a unique pair of solution $(u_h, \kappa_h) \in X_h \times M_h$ (cf. [8]). With $N = \dim(X_h)$, let $X_h = \text{span}\{\phi_1, \dots, \phi_N\}$ and $U = [x_1, \dots, x_N]'$ are the components of

$$u_h = \sum_{i=1}^N x_i \phi_i \in X_h.$$

Let E_1, E_2, E_3 be the edges of the triangle T , and let v_{E_k} denote the unit normal vector of E_k chosen with a global fixed orientation while v_k denotes the outer unit normal of T along E_k . We define the basis functions ψ_E of M_h , where $E \in \mathcal{E}^h / \mathcal{E}_N^h$ as below:

$$\psi_{E_k}(x) = \sigma_k \quad \text{for } k = 1, 2, 3 \text{ and } x \in T,$$

where $\sigma_k = v_{E_k} \cdot v_k$ is $+1$ if v_{E_k} points outward and otherwise -1 . Globally, let for any edge $E = T_+ \cap T_- \in \mathcal{E}_\Omega^h$

$$\psi_E(x) = \begin{cases} 1 & \text{for } x \in T_+, \\ -1 & \text{for } x \in T_-, \\ 0 & \text{elsewhere;} \end{cases}$$

and for $E \in \mathcal{E}_D^h$

$$\psi_E(x) = \begin{cases} 1 & \text{for } x \in E, \\ 0 & \text{elsewhere.} \end{cases}$$

With $L = \dim(M_h)$, let $M_h = \text{span}\{\psi_l\}_1^L$ with $\psi_l = \psi_{E_l}$, where $l = 1, \dots, L$ is an enumeration of edges

$$\mathcal{E}_\Omega^h \cup \mathcal{E}_D^h = \{E_1, \dots, E_L\}.$$

Let $\Lambda = [x_{N+1}, \dots, x_{N+L}]'$ are the components of κ_h such that

$$\kappa_h = \sum_{l=1}^L x_{N+l} \psi_l.$$

The problem (3.7)-(3.8) can be written in a linear system of equations for unknowns U and Λ as: for $j = 1, \dots, N$ and $l = 1, \dots, L$.

$$\begin{aligned} \sum_{i=1}^N x_i \sum_{T \in \mathcal{T}_h} \int_T ((A \nabla \phi_j + \phi_j p) \cdot \nabla \phi_i + \delta \phi_j \phi_i) \, dx - \sum_{l=1}^L x_{N+l} \int_{E_l} \psi_l [[\phi_j]]_{E_l} \, d\gamma \\ = \sum_{T \in \mathcal{T}_h} \int_T f \phi_j \, dx + \int_{\Gamma_N} g \phi_j \, d\gamma, \end{aligned} \quad (3.9)$$

$$-\sum_{i=1}^N x_i \int_{E_l} \psi_l [[\phi_i]]_{E_l} d\gamma = - \int_{E_l} \psi_l u_{Dh} d\gamma. \quad (3.10)$$

3.3 Local matrices $\mathbb{B}_T, \mathbb{D}_T, \mathbb{C}_T, \mathbb{M}_T$

With local numbers $i \in \{1, 2, 3\}$, let $\{a_i\}_{i=1}^3$ be the set of vertices of an element $T \in \mathcal{T}_h$ and $\{\lambda_i(x)\}_{i=1}^3$ be the set of barycentric coordinates of a point $x \in T$ (cf. [15]). Let $\{\phi_i^T(x)\}_{i=1}^3$ be the set of basis functions of $P_1(T)$. It should be noted that the basis functions of X_h are not globally continuous over Ω but locally continuous, which means that for any triangle $T \in \mathcal{T}_h$ with global node numbers i, j, k , $\phi_i = \lambda_1^T; \phi_j = \lambda_2^T; \phi_k = \lambda_3^T$.

Definition 3.1. The local matrices are defined for $i, j, l = 1, 2, 3$ as follows:

$$\begin{aligned} (\mathbb{B}_T)_{ji} &= \int_T A \nabla \phi_j \cdot \nabla \phi_i \, dx, & (\mathbb{D}_T)_{ji} &= \int_T (\phi_j p) \cdot \nabla \phi_i \, dx, \\ (\mathbb{C}_T)_{lj} &= \int_{E_l} \psi_l [[\phi_j]]_{E_l} \, d\gamma, & (\mathbb{M}_T)_{ji} &= \int_T \delta \phi_j \phi_i \, dx. \end{aligned}$$

The elaborate computation provides forms of all local matrices:

$$\mathbb{B}_T = |T| \begin{pmatrix} (A \nabla \lambda_1^T) \cdot \nabla \lambda_1^T & (A \nabla \lambda_1^T) \cdot \nabla \lambda_2^T & (A \nabla \lambda_1^T) \cdot \nabla \lambda_3^T \\ (A \nabla \lambda_2^T) \cdot \nabla \lambda_1^T & (A \nabla \lambda_2^T) \cdot \nabla \lambda_2^T & (A \nabla \lambda_2^T) \cdot \nabla \lambda_3^T \\ (A \nabla \lambda_3^T) \cdot \nabla \lambda_1^T & (A \nabla \lambda_3^T) \cdot \nabla \lambda_2^T & (A \nabla \lambda_3^T) \cdot \nabla \lambda_3^T \end{pmatrix}, \quad (3.11)$$

$$\mathbb{D}_T = \frac{|T|}{3} \begin{pmatrix} p \cdot \nabla \lambda_1^T & p \cdot \nabla \lambda_1^T & p \cdot \nabla \lambda_1^T \\ p \cdot \nabla \lambda_2^T & p \cdot \nabla \lambda_2^T & p \cdot \nabla \lambda_2^T \\ p \cdot \nabla \lambda_3^T & p \cdot \nabla \lambda_3^T & p \cdot \nabla \lambda_3^T \end{pmatrix}, \quad (3.12)$$

$$\mathbb{M}_T = \delta \begin{pmatrix} \int_T \lambda_1^T \lambda_1^T \, dx & \int_T \lambda_1^T \lambda_2^T \, dx & \int_T \lambda_1^T \lambda_3^T \, dx \\ \int_T \lambda_2^T \lambda_1^T \, dx & \int_T \lambda_2^T \lambda_2^T \, dx & \int_T \lambda_2^T \lambda_3^T \, dx \\ \int_T \lambda_3^T \lambda_1^T \, dx & \int_T \lambda_3^T \lambda_2^T \, dx & \int_T \lambda_3^T \lambda_3^T \, dx \end{pmatrix} = \delta |T| \begin{pmatrix} \frac{1}{6} & \frac{1}{12} & \frac{1}{12} \\ \frac{1}{12} & \frac{1}{6} & \frac{1}{12} \\ \frac{1}{12} & \frac{1}{12} & \frac{1}{6} \end{pmatrix}, \quad (3.13)$$

$$\mathbb{C}_T = \begin{pmatrix} \int_{E_1} \psi_1 [[\lambda_1^T]]_{E_1} \, d\gamma & \int_{E_1} \psi_1 [[\lambda_2^T]]_{E_1} \, d\gamma & \int_{E_1} \psi_1 [[\lambda_3^T]]_{E_1} \, d\gamma \\ \int_{E_2} \psi_2 [[\lambda_1^T]]_{E_2} \, d\gamma & \int_{E_2} \psi_2 [[\lambda_2^T]]_{E_2} \, d\gamma & \int_{E_2} \psi_2 [[\lambda_3^T]]_{E_2} \, d\gamma \\ \int_{E_3} \psi_3 [[\lambda_1^T]]_{E_3} \, d\gamma & \int_{E_3} \psi_3 [[\lambda_2^T]]_{E_3} \, d\gamma & \int_{E_3} \psi_3 [[\lambda_3^T]]_{E_3} \, d\gamma \end{pmatrix} = \begin{pmatrix} |E_1| \sigma_1 R_1 \\ |E_2| \sigma_2 R_2 \\ |E_3| \sigma_3 R_3 \end{pmatrix}, \quad (3.14)$$

where $R_1 = [0, \frac{1}{2}, \frac{1}{2}]$, $R_2 = [\frac{1}{2}, 0, \frac{1}{2}]$, $R_3 = [\frac{1}{2}, \frac{1}{2}, 0]$.

3.4 Right-hand side and boundary conditions

The computation of the right-hand side in (3.9)-(3.10) includes numerical integration over elements and edges of the functions f , g , and u_D . The right-hand side $F = \{F_j\}_{j=1}^N$ in (3.9) is defined as $F_j = b_j + LN_j$, where $b_j = \sum_{T \in \mathcal{T}_h} \int_T f \phi_j \, dx$ and $LN_j = \sum_{E \in \mathcal{E}_N^h} \int_E g \phi_j \, d\gamma$. Both parts are approximated by

$$b_j \approx \sum_{T \in \mathcal{T}_h} \frac{|T|}{3} \sum_{i=1}^3 f(m_{E_i}) \phi_j(m_{E_i}), \quad (3.15)$$

$$LN_j \approx \sum_{E \in \mathcal{E}_N^h} |E| g(m_E) \phi_j(m_E), \quad \text{where } m_E \in \mathcal{N}_m(\Gamma_N). \quad (3.16)$$

The right hand side $b_D = \{b_{D_l}\}_{l=1}^L$ in (3.10) is defined and approximated as

$$\begin{aligned} b_{D_l} &= - \int_{E_l} \psi_l u_{Dh} \, d\gamma \\ &\approx -|E_l| \sigma_l u_{Dh}(m_{E_l}), \quad \text{where } m_{E_l} \in \mathcal{N}_m(\Gamma_D) \\ &\approx -|E_l| u_{Dh}(m_{E_l}), \quad \text{since } \sigma_l = 1 \text{ for } l = 1, \dots, L. \end{aligned} \quad (3.17)$$

3.5 Assembly of the global matrices

In vector-matrix form, (3.9)-(3.10) can be written as

$$\mathbf{M}_{\text{vec}} \mathbf{W}_{\text{vec}} = \mathbf{F}_{\text{vec}}, \quad (3.18)$$

where global matrices and vectors read

$$\begin{aligned} \mathbf{M}_{\text{vec}} &= \begin{pmatrix} \mathbb{B} + \mathbb{D} + \mathbb{M} & -\mathbb{C}' \\ -\mathbb{C} & 0 \end{pmatrix}_{(N+L) \times (N+L)}, \quad \mathbf{W}_{\text{vec}} = \begin{pmatrix} \mathbf{U} \\ \Lambda \end{pmatrix}_{(N+L) \times 1}, \quad \mathbf{F}_{\text{vec}} = \begin{pmatrix} \mathbf{F} \\ b_D \end{pmatrix}_{(N+L) \times 1}, \\ \mathbb{B} &= (\mathbb{B}_{ij})_{N \times N}, \quad \mathbb{B}_{ij} = \sum_{T \in \mathcal{T}_h} \int_T (A \nabla \phi_i) \cdot \nabla \phi_j \, dx, \\ \mathbb{D} &= (\mathbb{D}_{ij})_{N \times N}, \quad \mathbb{D}_{ij} = \sum_{T \in \mathcal{T}_h} \int_T (\phi_i p) \cdot \nabla \phi_j \, dx, \\ \mathbb{M} &= (\mathbb{M}_{ij})_{N \times N}, \quad \mathbb{M}_{ij} = \sum_{T \in \mathcal{T}_h} \int_T \phi_i \cdot \phi_j \, dx, \\ \mathbb{C} &= (\mathbb{C}_{N+l,i})_{L \times N}, \quad \mathbb{C}_{N+l,i} = \int_{E_l} \psi_l [[\phi_i]]_{E_l} \, d\gamma, \\ \mathbf{F} &= (F_j)_{N \times 1}, \quad b_D = (b_{D_l})_{L \times 1}. \end{aligned}$$

3.6 Implementation

MATLAB code of vectorized StiffMassConv_PH.m

Here we explain the vectorized code **StiffMassConv_PH.m**, where we compute the matrices \mathbb{B} , \mathbb{D} , $\mathbb{M} \in \mathbb{R}^{N \times N}$, and $b \in \mathbb{R}^{N \times 1}$. The vectorization of stiffness matrix \mathbb{B} and load vector b are similar to the MATLAB code Listing 3 in [5] with an adequate amount of modifications.

```

1 function [B,D,M,b]=StiffMassConv_PH(coordinates,elements,params)
2 A=params.A;p=params.p;delta=params.delta;
3 nE=size(elements,1); % number of elements
4 %% Vectorization of B matrix
5 P1=coordinates(elements(:,1,:)); % collection of the first nodes of all triangles
6 P2=coordinates(elements(:,2,:)); % collection of the second nodes of all triangles
7 P3=coordinates(elements(:,3,:)); % collection of the third nodes of all triangles
8 d21=P2-P1; d31=P3-P1; d32=P3-P2; % represents the edges of the elements in a
9 mesh
10 mp23=1/2.* (P2+P3); mp13=1/2.* (P1+P3); mp12=1/2.* (P1+P2); % midpoints of the
11 edges
12 area4=2*(d21(:,1).*d31(:,2)-d21(:,2).*d31(:,1)); % 4*Area
13 GI=reshape([1:3*nE; 1:3*nE; 1:3*nE],9,nE); % 3*nE =Number of nodes
14 I3=reshape(GI([1 4 7 2 5 8 3 6 9],:),9*nE,1);
15 J3=reshape(GI,9*nE,1);
16 a3=(sum(([d21(:,2),d21(:,1)]*A).*[d31(:,2),d31(:,1)],2)./area4)';
17 b3=(sum(([d31(:,2),d31(:,1)]*A).*[d31(:,2),d31(:,1)],2)./area4)';
18 c3=(sum(([d21(:,2),d21(:,1)]*A).*[d21(:,2),d21(:,1)],2)./area4)';
19 BT=[-2*a3+b3+c3; a3-b3; a3-c3; a3-b3;b3;-a3;a3-c3;-a3;c3];
20 B=sparse(I3,J3,BT,3*nE,3*nE);
21 %% Vectorization of mass matrix (M)
22 MT=reshape(delta.*(area4./48).*[2;1;1;1;2;1;1;1;2],9*nE,1);
23 M=sparse(I3,J3,MT,3*nE,3*nE);
24 %% Vectorization of D matrix
25 h1=(-p(1)*d32(:,2)+p(2)*d32(:,1))./6;
26 h2=(p(1)*d31(:,2)-p(2)*d31(:,1))./6;
27 h3=(-p(1)*d21(:,2)+p(2)*d21(:,1))./6;
28 DT=[ h1; h1; h1; h2; h2; h2; h3; h3; h3];
29 D=sparse(I3,J3,DT,3*nE,3*nE);
30 %% Vectorization of load vector b
31 f1=f(mp13,params)./2 +f(mp12,params)./2;
32 f2=f(mp23,params)./2+f(mp12,params)./2;
33 f3=f(mp13,params)./2+f(mp23,params)./2;
34 fT=(area4.*[f1 f2 f3])./12;
35 b = accumarray (reshape(1:3*nE,3*nE,1), reshape(fT',3*nE,1) ,[3*nE 1]);
36 end

```

Listing 5: Vectorization of the assembly of stiffness matrix \mathbb{B} , convection matrix \mathbb{D} , mass matrix \mathbb{M} and load vector b .

- Line 11-13: We create a $9 \times nE$ matrix called GI by reshaping the matrix $[1 : 3 \times nE; 1 : 3 \times nE; 1 : 3 \times nE]$ such that each column of GI (cf. Fig. 5) corresponds to the column index of local stiffness matrices for elements in the global assembly. $I3$ and $J3$ (cf. Fig. 6) contain index pairs for the global stiffness matrix, constructed using GI . Note that, $I3$ is based on the modified GI with specific row indices $[1 4 7 2 5 8 3 6 9]$, while $J3$ is based on the original GI .

Define, the row and column index pair of entries in the stiffness matrix corresponding

to the m^{th} element as

$$\rho(m) = \begin{bmatrix} 3(m-1)+1 \\ 3(m-1)+2 \\ 3(m-1)+3 \\ 3(m-1)+1 \\ 3(m-1)+2 \\ 3(m-1)+3 \\ 3(m-1)+1 \\ 3(m-1)+2 \\ 3(m-1)+3 \end{bmatrix} \quad \text{and} \quad \theta(m) = \begin{bmatrix} 3(m-1)+1 \\ 3(m-1)+1 \\ 3(m-1)+1 \\ 3(m-1)+2 \\ 3(m-1)+2 \\ 3(m-1)+3 \\ 3(m-1)+3 \\ 3(m-1)+3 \\ 3(m-1)+3 \end{bmatrix}, \quad \text{where } m = 1, 2, \dots, nE.$$

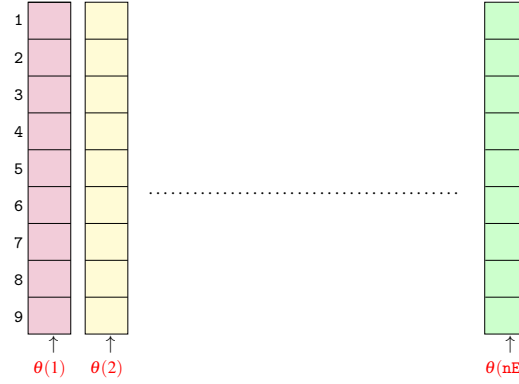


Fig. 5: Geometrical representation of the columns of the GI matrix in MATLAB.

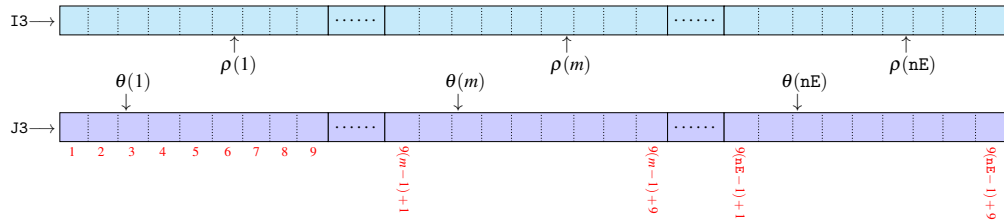


Fig. 6: Geometrical representation of I3 and J3 column vectors in MATLAB.

Remark 2. The index pair vectors for conforming (cf. [5]) and non-conforming FEM differ in vectorization because of the distinct element-wise assembly of the local stiffness matrices. For primal hybrid FEM, we generate I3 and J3 index pair vectors that are compatible with non-conforming P1-FEM.

- Line 14-18: The vectors $a3$, $b3$, and $c3$ for element T are

$$a3|_T = \frac{1}{4|T|} ([y_2 - y_1 \ x_2 - x_1] A) \cdot [y_3 - y_1 \ x_3 - x_1], \quad (3.19)$$

$$b3|_T = \frac{1}{4|T|} ([y_3 - y_1 \ x_3 - x_1] A) \cdot [y_3 - y_1 \ x_3 - x_1], \quad (3.20)$$

$$c3|_T = \frac{1}{4|T|} ([y_2 - y_1 \ x_2 - x_1] A) \cdot [y_2 - y_1 \ x_2 - x_1]. \quad (3.21)$$

- Line 19-21: The element-wise assembly of \mathbb{M} uses nine updates of the mass matrix per element T . That is, the vector MT has length $9 \times nE$.
- Lines 22-27: $h1|_T$, $h2|_T$, and $h3|_T$ are entries of the matrix \mathbb{D}_T (3.12),

$$h1|_T = \frac{1}{6} p \cdot \begin{bmatrix} -(y_3 - y_2) \\ x_3 - x_2 \end{bmatrix}, \quad h2|_T = \frac{1}{6} p \cdot \begin{bmatrix} y_3 - y_1 \\ -(x_3 - x_1) \end{bmatrix}, \quad h3|_T = \frac{1}{6} p \cdot \begin{bmatrix} -(y_2 - y_1) \\ x_2 - x_1 \end{bmatrix}.$$

We assemble the convection matrix \mathbb{D} by using **sparse** command in MATLAB with $I3$ (row index) and $J3$ (column index).

- Line 28-33: We evaluate the volume forces $f(m_{E_i})$, $i = 1, 2, 3$ for all triangle $T \in \mathcal{T}_h$, then (3.15) and assemble the load vector b using **accumarray**.

MATLAB code of Vectorized Lambda_PH.m

```

1  function [C,e11,v,R11]= Lambda_PH(coordinates,ed2el,intE,Dbed,Redges,led,ledTN)
2  nrEdges=size(ed2el,1); % number of edges
3  num_intE=size(intE,1); % number of interior edges
4  nDb=size(Dbed,1); % number of Dirichlet boundary edges
5  edges=ed2el(1:nrEdges,1:2); % all edges
6  %% Vectorization of matrix C
7  v=vecnorm((coordinates(edges(:,1),:)-coordinates(edges(:,2),:))'); % length of
8  edges
9  e11=ed2el(:,3); e12=nonzeros(ed2el(:,4));
10 i=find(led==1); j=find(led==2); k=find(led==3);
11 p=find(ledTN(intE)==1); q=find(ledTN(intE)==2); r=find(ledTN(intE)==3);
12 R1=[0, 1/2, 1/2]; R2= [1/2, 0, 1/2]; R3= [1/2, 1/2, 0];
13 R11(i,:)=repmat(R1,size(i));
14 R11(j,:)=repmat(R2,size(j));
15 R11(k,:)=repmat(R3,size(k));
16 R22(p,:)=repmat(R1,size(p));
16 R22(q,:)=repmat(R2,size(q));
17 R22(r,:)=repmat(R3,size(r));
18 I1=reshape([Dbed' intE';Dbed' intE';Dbed' intE'],3*(num_intE+nDb),1);
19 J1=reshape(((e11([Dbed' intE'])-ones(num_intE+nDb,1))*3+[1 2 3])'...
20 ,3*(num_intE+nDb),1);
21 S1=reshape(( v([Dbed' intE']).* R11([Dbed' intE']),:)),3*(num_intE+nDb),1);
22 I2=reshape([intE';intE';intE'],3*num_intE,1);
23 J2=reshape(((e12(:)-ones(num_intE,1)).*3+[1 2 3]),3*num_intE,1);
24 S2=reshape((-1).*v(intE).*(R22)'),3*num_intE,1);
25 I=[I1;I2]; J=[J1;J2]; S=[S1;S2]; % appending vectors
26 C=sparse(I, J, S);
27 C=C(Redges, :); % eliminate extra rows
28 end

```

Listing 6: Vectorized and efficient MATLAB implementation of the assembly of matrix \mathbb{C} .

- Line 1: The function **Lambda_PH.m** takes the coordinates data, $ed2el$, $intE$, Dirichlet boundary edges($Dbed$), $Redges$ ($\mathcal{E}^h/\mathcal{E}_N^h$), led , and $ledTN$. It computes the matrix $\mathbb{C} \in$

$\mathbb{R}^{L \times N}$ in (3.18) and other required data $e11$, v , $R11$ for **Main.m** described in the next subsection.

- Line 7-8: The length of all edges is computed by using the MATLAB function **vecnorm** and stored in a vector v . Vector $e11 = \text{ed2el}(:, 3)$, which contains the index of all T_+ elements, and vector $e12 = \text{nonzeros}(\text{ed2el}(:, 4))$, which contains the index of all T_- elements.
- Line 9-10: For each triangular element $T_+ \in \mathcal{T}_h$, the vectors i, j, k store the indices of the first edge (E_1), second edge (E_2), third edge (E_3), respectively. Similarly, the vectors p, q, r store the indices of E_1, E_2, E_3 for T_- elements.
- Line 11-17: We construct the matrices $R11 \in \mathbb{R}^{L \times 3}$ and $R22 \in \mathbb{R}^{N_\Omega \times 3}$ based on the values of the led and ledTN vectors, as well as the R_1, R_2 , and R_3 vectors (Definition 3.1). The rows of $R11$ corresponding to E_1, E_2 , and E_3 of each $T_+ \in \mathcal{T}_h$ are populated with the vectors R_1, R_2 , and R_3 , respectively. This is accomplished by using the **repmat** function to replicate each vector along the rows of $R11$ at the indices stored in i, j , and k , respectively. Similarly, for each $T_- \in \mathcal{T}_h$, we build the rows of $R22$ are R_1, R_2 , and R_3 vectors with respect to the indices stored in p, q , and r .
- Line 18-24: We calculate the row and column indexing vectors $I1$ and $J1 \in \mathbb{R}^{3L \times 1}$ (as shown in Fig. 7) for the matrix \mathbb{C} based on the T_+ elements. Similarly, we obtain the row and column indexing vectors $I2$ and $J2 \in \mathbb{R}^{3N_\Omega \times 1}$ (as shown in Fig. 8) for the matrix \mathbb{C} based on the T_- elements. The entries of matrix \mathbb{C} corresponding to T_+ and T_- elements are represented by $S1 \in \mathbb{R}^{3L \times 1}$ (as shown in Fig. 7) and $S2 \in \mathbb{R}^{3N_\Omega \times 1}$ (as shown in Fig. 8), respectively, and are arranged in column vectors:

$$S1|_{T_+} = \begin{pmatrix} v(i) R11(i,:) \\ v(j) R11(j,:) \\ v(k) R11(k,:) \end{pmatrix}, \text{ where } i, j, \text{ and } k \text{ are the global edge number of } T_+,$$

$$\text{and } S2|_{T_-} = \begin{pmatrix} -v(p) R22(p,:) \\ -v(q) R22(q,:) \\ -v(r) R22(r,:) \end{pmatrix}, \text{ where } p, q, \text{ and } r \text{ are the global edge number of } T_-.$$

Let $\alpha_1, \alpha_2, \dots, \alpha_{N_D}$ be the global numbers of the \mathcal{E}_D^h for the mesh \mathcal{T}_h . Let $\beta_1, \beta_2, \dots, \beta_{N_\Omega}$ be global numbers of \mathcal{E}_Ω^h for the mesh \mathcal{T}_h . Define,

$$\gamma_m = (e11(m) - 1) * 3 + [1 2 3], \text{ where } m = 1, 2, \dots, \text{nrEdges},$$

$$\text{and } \zeta_l = (e12(l) - 1) * 3 + [1 2 3], \text{ where } l = 1, 2, \dots, N_\Omega.$$

- Line 25-27: We are appending the vectors $I=[I1; I2]$, $J=[J1; J2]$, $S=[S1; S2]$. We assemble the matrix \mathbb{C} by using **sparse** with I, J , and S , but it has extra zero rows with respect to the \mathcal{E}_N^h . We eliminate the extra rows from matrix \mathbb{C} in line 27.

MATLAB code of Main.m

```

1 load('coordinates.dat');    load('elements.dat');
2 load('Dirichlet.dat');    load('Neumann.dat');
3 [n2el,n2ed,ed2el,intE,extE,led,ledTN]=edge_vec(elements,coordinates);
4 params.A=[1 0; 0 1]; params.p=[1,1]; params.delta=1; % problem parameters

```

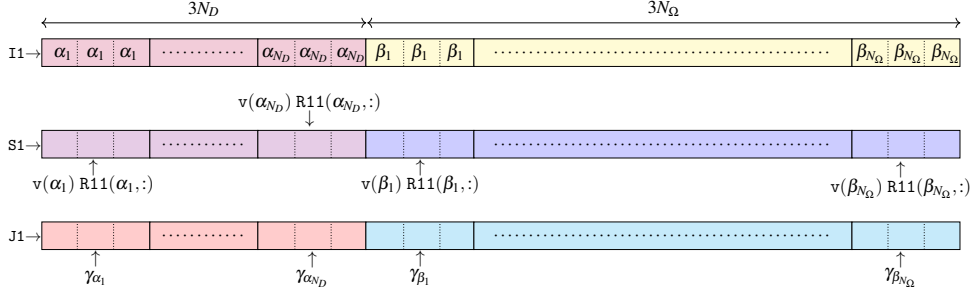


Fig. 7: Geometrical representation of I1, J1, and S1 vectors in MATLAB.

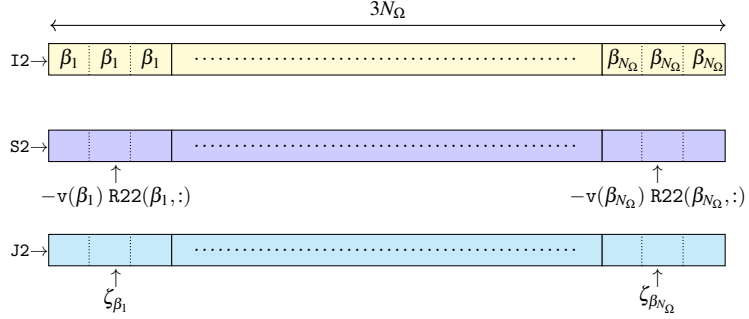


Fig. 8: Geometrical representation of I2, J2, and S2 vectors in MATLAB.

```

5 nt=4;
6 for p1=1:nt
7   fprintf('Level = %d\n',p1);
8   tic
9   [coordinates,elements,Dirichlet,Neumann]=redrefine_vec(coordinates,elements,
10   n2ed,ed2el,Dirichlet,Neumann);
11   fprintf('run-time(in sec) for the function redrefine_vec.m is = %d\n',toc);
12   tic
13   [n2el,n2ed,ed2el,intE,extE,led,ledTN]=edge_vec(elements,coordinates);
14   fprintf('run-time(in sec) for the function edge_vec.m is = %d\n',toc);
15   h(p1)=sqrt(det([1 1;coordinates(elements(1,:),:,:)'])*2); % space parameter
16   grad4e = getGrad4e(coordinates,elements);
17   nrEdges=size(ed2el,1); % Number of Edges
18   Dbed= diag(n2ed(Dirichlet(:,1),Dirichlet(:,2))); %Dirichlet boundary edges
19   Nbed= diag(n2ed(Neumann(:,1),Neumann(:,2))); %Neumann boundary edges
20   Redges=setdiff(1:nrEdges,Nbed); % removing Neumann edges from all edges
21   L=length(Redges);
22   nE=size(elements,1); % number of elements
23   fprintf('number of elements = %d\n',nE);
24   ndf=3*nE; %degree of freedom
25   tic
26   [B,D,M,b]=StiffMassConv_PH(coordinates,elements,params);
27   fprintf('run-time(in sec) for the function StiffMassConv_PH.m is = %d\n',toc);
28   tic
29   [C,e11,v,R11]= Lambda_PH(coordinates,ed2el,intE,Dbed,Redges,led,ledTN);
30   fprintf('run-time(in sec) for the function Lambda_PH.m is = %d\n',toc);
31   %% Vectorization of Neumann BC
32   LN=sparse(ndf,1);
33   if (~isempty(Neumann))
34     nNb=size(Nbed,1); % number of Neumann boundary edges
35     NP1=coordinates(Neumann(:,1,:)); NP2=coordinates(Neumann(:,2),:);
      Nmd=1/2.* (NP1+NP2); % mid-point of Neumann edges

```

```

36      Nnorm=[NP2(:,2)-NP1(:,2) NP1(:,1)-NP2(:,1)]./vecnorm((NP1-NP2)'); %normal
37      to Neumann edge
38      JN=reshape(((e11(Nbed)-ones(nNb,1))*3+[1 2 3]),3*nNb,1);
39      S=reshape(((diag(v(Nbed).*g(Nmd,nE,params)*Nnorm')).*R11(Nbed,:)),3*nNb,1)
40      ;
41      LN= accumarray (JN, S ,[ndf 1]);
42      end
43      %% Dirichlet boundary condition
44      uhb1=sparse(L,1);
45      if (~isempty(Dirichlet))
46          [ed,~]=find(Redges==Dbed); % extract the linear indices of Dirichlet edge
47          number
48          me=(coordinates(Dirichlet(:,2),:)+coordinates(Dirichlet(:,1),:))./2; % mid-
49          point of Dirichlet edges
50          uhb1(ed)=-v(Dbed).*uD(me);
51      end
52      %%%%%% Solving saddle point problem %%%%%%
53      Mvec=[ B + D + M -C';
54          -C sparse(L,L)];
55      Fvec=[b+LN ; uhb1];
56      Wvec=Mvec\ Fvec;
57      uh=Wvec(1:ndf);
58      Kh=Wvec(1+ndf:length(Wvec));
59      u=ue(coordinates(elements',:),nE,1); % exact solution
60      K=exactLambda(elements,coordinates,ed2el,e11,led,Redges,params);
61      tic
62      [H1e(p1),L2e(p1),Merr(p1)]=PHerror(uh,C,B,Kh,K,grad4e,elements,coordinates);
63      fprintf('run-time(in sec) for the function PHerror.m is = %d\n',toc);
64      end
65      %% order of convergence
66      for j=1:p1-1
67          ocl2(j)=log(L2e(j)/L2e(j+1))/log(h(j)/h(j+1));
68          och1(j)=log(H1e(j)/H1e(j+1))/log(h(j)/h(j+1));
69          ocm(j)=log(Merr(j)/Merr(j+1))/log(h(j)/h(j+1));
70      end
71      fprintf('order of convergences w.r.t h \n in      H1-norm      L2-norm      M-norm \n');
72      disp([och1',ocl2',ocm']);
73

```

Listing 7: **Main.m**.

- The computation of $LN \in \mathbb{R}^{N \times 1}$ in MATLAB reads lines 31-40, incorporating the Neumann boundary conditions. The Neumann boundary condition in (3.16) at every midpoint $me \in \mathcal{N}_m(\Gamma_N)$ is evaluated. JN and $S \in \mathbb{R}^{3N_n \times 1}$ (Fig. 9) indicate the row indexing vector and entries for the matrix LN . Let $\eta_1, \eta_2, \dots, \eta_{N_n}$ be the Neumann boundary edge global numbers for the mesh \mathcal{T}_h .

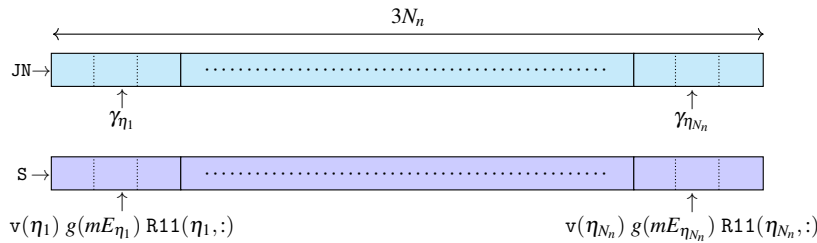


Fig. 9: Geometrical representation of JN , and S vectors in MATLAB.

The assembly of the matrix LN is done in line 39 by using the **accumarray** with JN and S .

- Line 42-47: In taking care the Dirichlet boundary condition (3.17), the integral is approximated by the mid-point rule.
- Line 49-51: Assembly of M_{vec} (see, (3.18)) in which zero ($L \times L$) matrix defined as a **sparse** matrix, which helps to save run-time and storage space for zero-valued entries.
- Line 56: The κ (3.6) is calculated using the **exactLambda.m** function.
- Line 58: The errors $u - u_h$ and $\kappa - \kappa_h$ over X and M are computed using the **PHerror.m** function.

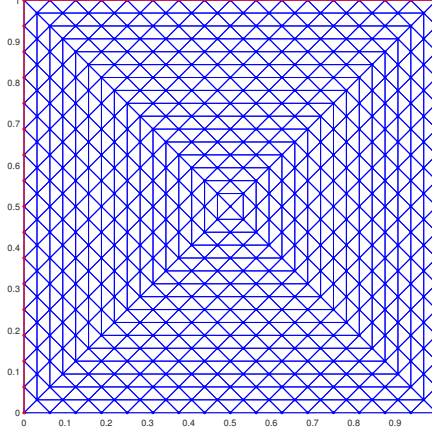


Fig. 10: Example of (level 4, $h = 1/16$) red-refined mesh used in computations of both elliptic and parabolic models. Red-colored sides denote Γ_N .

Example 2. Let $A = I_{2 \times 2}$, $p = [1, 1]$, $\delta = 1$. In (3.1)-(3.3) we take the exact solution

$$u(x_1, x_2) = (x_1 - x_1^2)(x_2 - x_2^2)$$

defined on $\Omega = (0, 1) \times (0, 1)$ and corresponding to the load function f in the form

$$f(x_1, x_2) = 2(x_2 - x_2^2) + 2(x_1 - x_1^2) + (1 - 2x_1)(x_2 - x_2^2) + (x_1 - x_1^2)(1 - 2x_2) + u(x_1, x_2).$$

The Dirichlet boundary condition reads

$$u_D = 0 \quad \text{on } \Gamma_D$$

and the Neumann boundary condition.

$$g(x_1, x_2) = [(1 - x_1 - x_1^2)(x_2 - x_2^2), (x_1 - x_1^2)(1 - x_2 - x_2^2)] \cdot \nu \quad \text{on } \Gamma_N,$$

where ν denotes the outer normal vector (cf. Fig. 10).

Table 3 Run-time of the **StiffMassConv_PH.m** and **Lambda_PH.m** for second order elliptic model problem.

Level	nE	run-time (in sec)	
		StiffMassConv_PH.m	Lambda_PH.m
4	1024	0.0029	0.0035
5	4096	0.01	0.017
6	16384	0.018	0.025
7	65536	0.071	0.11
8	262144	0.3	0.51
9	1048576	1.23	2.13
10	4194304	5.60	9.25

Table 3 displays the runtime (in seconds) for vectorized implementations of functions **StiffMassConv_PH.m** and **Lambda_PH.m**, which vary with the number of elements in the mesh.

In Fig. 11, we performed a linear regression analysis for the runtime of **StiffMassConv_PH.m** (left) and **Lambda_PH.m** (right) with respect to the number of elements. We obtained an R-squared approximately equal to 1 in both cases, concluding that our MATLAB implementations are of nearly linear time-scaling.

In Table 4, the errors $u - u_h$ in the L^2 and H^1 -norm, and the error $\kappa - \kappa_h$ in M -norm over space M are presented. In addition, we present the order of convergence in the respective norms.

Table 4 Order of convergence in L^2 , H^1 and M -norms for second order elliptic model problem.

Level	$\ u - u_h\ _{H^1}$	Order of convergence	$\ u - u_h\ _{L^2}$	Order of convergence	$\ \kappa - \kappa_h\ _M$	Order of convergence
1	0.0801		0.0109		0.0232	
2	0.0397	1.0125	0.0025	2.1050	0.0107	1.1219
3	0.0197	1.0083	6.22e-04	2.0309	0.0055	0.9678
4	0.0099	1.0023	1.54e-04	2.0079	0.0028	0.9866
5	0.0049	1.0006	3.86e-05	2.0020	0.0014	0.9963

4 Implementation of second order parabolic model problem

4.1 Parabolic problem and algebraic formulation

Consider a second-order parabolic model problem with mixed boundary condition

$$u_t(x, t) - \nabla \cdot (A \nabla u + up) + \delta u = f(x, t) \quad \text{in } \Omega \times (0, t_{\bar{N}}], \quad (4.1)$$

$$u(x, t) = u_D(x, t) \quad \text{on } \Gamma_D \times (0, t_{\bar{N}}], \quad (4.2)$$

$$(A \nabla u + ub) \cdot v = g(x, t) \quad \text{on } \Gamma_N \times (0, t_{\bar{N}}] \quad (4.3)$$

$$u(x, 0) = u_0(x) \quad \text{in } \Omega, \quad (4.4)$$

where f , g and u_0 are appropriate smooth functions. Primal hybrid formulation of (4.1)-(4.4) is to seek a pair of solutions $(u, \kappa) : [0, t_{\bar{N}}] \rightarrow X \times M$ such that

$$(u_t, v) + a(u, v) + b(v, \kappa) = (f, v) + \langle g, v \rangle_{\Gamma_N}, \quad \forall v \in X, \quad (4.5)$$

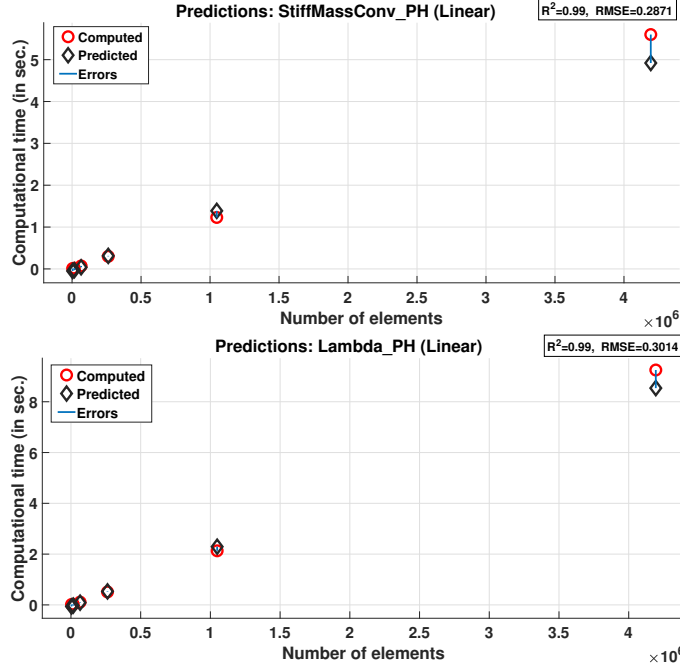


Fig. 11: Linear regression analysis between the computed and predicted values by Regression Learner (Statistics and Machine Learning Toolbox 11.7) in MATLAB.

$$b(u, \chi) = \langle u_D, \chi \rangle, \quad \forall \chi \in M, \quad (4.6)$$

$$u(0) = u_0, \quad (4.7)$$

Let the time interval $[0, t_{\tilde{N}}]$ be partitioned into equally spaced points

$$0 = t_0 < t_1 < \dots < t_{\tilde{N}}$$

with time step parameter k such that $\tilde{N} = t_{\tilde{N}}/k$ and $t_n = nk$ for $n \in \{1, 2, \dots, \tilde{N}\}$. For $\varphi \in \mathcal{C}[0, t_{\tilde{N}}]$, we set the backward difference operator ∂ as

$$\partial \varphi^n = (\varphi^n - \varphi^{n-1})/k$$

and for $t_{n-1/2} = (n - 1/2)k$ the midpoint value as

$$\varphi^{n-1/2} = (\varphi^n + \varphi^{n-1})/2.$$

By employing the Crank-Nicolson implicit scheme in the time direction, we seek a solution pair $(u_h^n, \kappa_h^n) \in X_h \times M_h$ satisfying

$$\sum_{T \in \mathcal{T}_h} \int_T \partial u_h^n v_h \, dx + \sum_{T \in \mathcal{T}_h} \int_T \nabla u_h^{n-1/2} \cdot \nabla v_h \, dx + \sum_{T \in \mathcal{T}_h} \int_T (u_h^{n-1/2} p) \cdot \nabla v_h \, dx$$

$$\begin{aligned}
& + \sum_{T \in \mathcal{T}_h} \int_T \delta u_h^{n-1/2} v_h \, dx - \sum_{E \in \mathcal{E}^h / \mathcal{E}_N^h} \int_E \kappa_h^{n-1/2} [[v_h]]_E \, d\gamma = F^{t_{n-1/2}}(v_h), \\
& - \sum_{E \in \mathcal{E}^h / \mathcal{E}_N^h} \int_E \chi_h [[u_h^{n-1/2}]]_E \, d\gamma = - \sum_{E \in \mathcal{E}^h / \mathcal{E}_N^h} \int_E \chi_h u_{Dh}^{n-1/2} \, d\gamma,
\end{aligned}$$

for any testing pair $(v_h, \chi_h) \in X_h \times M_h$. Here,

$$F^{t_{n-1/2}}(v_h) = \sum_{T \in \mathcal{T}_h} \int_T f(t_{n-1/2}) v_h \, dx + \sum_{E \in \mathcal{E}_N^h} \int_E g(t_{n-1/2}) v_h \, d\gamma.$$

Remark 3. For this implicit scheme, we obtain a second-order convergence for the primal variable in L^2 -norm (cf. [16]), one can construct a complete discrete setup using any other implicit or explicit scheme.

Using the matrices $\mathbb{M}, \mathbb{B}, \mathbb{D}$, and \mathbb{C} constructed for the elliptic case, we write the above algebraic formulation in matrix-vector form,

$$\mathbb{M}_+ \mathbf{W}^n = \mathbb{M}_- \mathbf{W}^{n-1} + \mathbf{F}. \quad (4.8)$$

Here,

$$\begin{aligned}
\mathbb{M}_\pm &= \begin{pmatrix} (1 \pm \frac{1}{2}k\delta)\mathbb{M} \pm \frac{1}{2}k\mathbb{B} \pm \frac{1}{2}k\mathbb{D} & \mp \frac{1}{2}k\mathbb{C}' \\ \mp \frac{1}{2}\mathbb{C} & 0 \end{pmatrix}_{(N+L) \times (N+L)}, \\
\mathbf{W}^n &= \begin{pmatrix} \mathbf{U}^n \\ \mathbf{\Lambda}^n \end{pmatrix}_{(N+L) \times 1}, \quad \mathbf{W}^{n-1} = \begin{pmatrix} \mathbf{U}^{n-1} \\ \mathbf{\Lambda}^{n-1} \end{pmatrix}_{(N+L) \times 1}, \\
\mathbf{F} &= \begin{pmatrix} kF^{n-1/2} \\ b_D^{n-1/2} \end{pmatrix}_{(N+L) \times 1}, \quad F^{n-1/2} = (F_j^{n-1/2})_{N \times 1}.
\end{aligned}$$

For global basis functions ϕ_j ,

$$F_j^{n-1/2} = b_j^{n-1/2} + LN_j^{n-1/2},$$

where

$$b_j^{n-1/2} \approx \sum_{T \in \mathcal{T}_h} \int_T f^{n-1/2} \phi_j \, dx, \quad LN_j^{n-1/2} \approx \sum_{E \in \mathcal{E}_N^h} \int_E g^{n-1/2} \phi_j \, d\gamma.$$

Then, $b_j^{n-1/2} = \frac{1}{2}b_j^{n-1} + \frac{1}{2}b_j^n \approx \sum_{T \in \mathcal{T}_h} \frac{1}{2} \int_T (f^{n-1} \phi_j + f^n \phi_j) \, dx$. Here, b_j^n is obtained as follows

$$b_j^n \approx \sum_{T \in \mathcal{T}_h} \frac{|T|}{3} \sum_{i=1}^3 f(m_{E_i}, t_n) \phi_j(m_{E_i}). \quad (4.9)$$

The Neumann boundary term $LN_j^{n-1/2} = (LN_j^{n-1} + LN_j^n)/2$, and LN_j^n is obtained by

$$LN_j^n \approx \sum_{E \in \mathcal{E}_N^h} |E| g(m_E, t_n) \phi_j(m_E), \quad \text{where } m_E \in \mathcal{N}_m(\Gamma_N). \quad (4.10)$$

The component related to the Dirichlet boundary $b_D^{n-1/2}$ is defined as follows

$$b_D^{n-1/2} = (b_{D_l}^{n-1/2})_{L \times 1}, \quad b_{D_l}^{n-1/2} \approx - \int_{E_l} \psi_l u_{Dh}^{n-1/2} d\gamma.$$

Similarly, we obtain $b_{D_l}^{n-1/2} = (b_{D_l}^{n-1} + b_{D_l}^n)/2$, and $b_{D_l}^n$ is obtained by

$$\begin{aligned} b_{D_l}^n &\approx - \int_{E_l} \psi_l u_{Dh}^n d\gamma \approx -|E_l| \sigma_l u_{Dh}^n(m_{E_l}), \quad \text{where } m_{E_l} \in \mathcal{N}_m(\Gamma_D) \\ &= -|E_l| u_{Dh}^n(m_{E_l}), \quad \text{since } \sigma_l = 1 \text{ for } l = 1, \dots, L. \end{aligned} \quad (4.11)$$

The functions **StiffMassConv_PH.m** and **Lambda_PH.m** for the parabolic model problem will be similar to those for the elliptic model problem, which will handle the assembly of the matrices \mathbb{M} , \mathbb{B} , \mathbb{C} , \mathbb{D} . But, for the Crank-Nicolson scheme, we need to compute the vector $F^{n-1/2}$ at $t_{n-1/2}$, it is achieved by evaluating at t_n and t_{n-1} time points then taking an average of them. This necessitates the utilization of another function **load_t.m** within **ParabolicMain.m**. The **load_t.m** calculates the values of b^n (4.9) and LN^n (4.10) at different time points t_n .

Example 3. We consider again $A = I_{2 \times 2}$, $p = [1, 1]$ $\delta = 1$ and the time interval $[0, 1]$. In (4.1)-(4.4) we take exact solution u and corresponding load function f in the forms

$$\begin{aligned} u(x_1, x_2, t) &= t(x_1 - x_1^2)(x_2 - x_2^2), \\ f(x_1, x_2, t) &= (x_1 - x_1^2)(x_2 - x_2^2) + 2t(x_2 - x_2^2) + 2t(x_1 - x_1^2) \\ &\quad + t(1 - 2x_1)(x_2 - x_2^2) + t(x_1 - x_1^2)(1 - 2x_2) + u(x_1, x_2, t). \end{aligned}$$

The Dirichlet and Neumann boundary (cf. Fig. 10) condition read $u_D = 0$ and

$$g(x_1, x_2) = [t(1 - x_1 - x_1^2)(x_2 - x_2^2), t(x_1 - x_1^2)(1 - x_2 - x_2^2)] \cdot v$$

Table 5 shows the error $u - u_h$ in the L^2 and H^1 -norms, and the error $\kappa - \kappa_h$ in the M -norm. For optimal order convergence of the Crank-Nicholson scheme, the space variable h and the time parameter k are considered equal, that is, $h = k$. Examples of particular exact and approximate solutions are shown in Figs. 12, 13.

5 Concluding remarks

Primal hybrid FEM has been implemented efficiently in MATLAB for general two-dimensional elliptic and parabolic problems with mixed boundary conditions. Numerical experiments show that the codes are of nearly linear time-scaling, and the method converges optimally. The presented codes are flexible and may be extended to non-linear

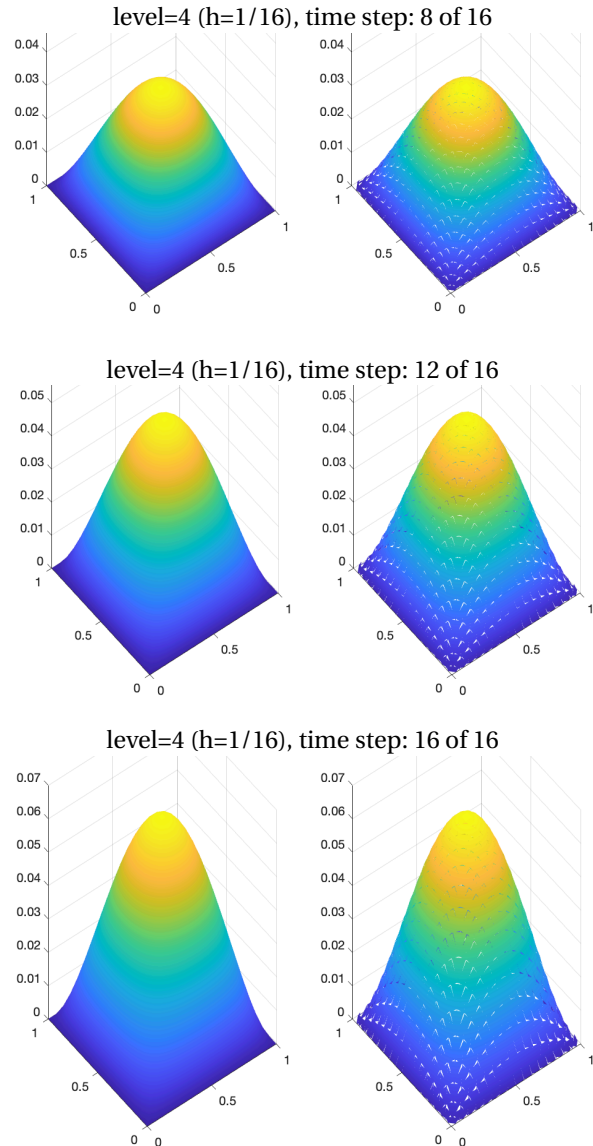


Fig. 12: Exact u (left column) vs. approximate u_h solutions from the broken Sobolev space (right column) of the parabolic model at selected time steps.

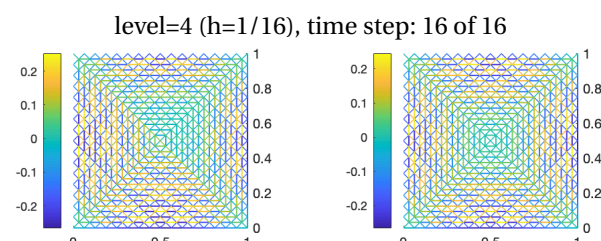


Fig. 13: Exact κ (left column) and approximate κ_h Lagrange multipliers (right column) of the parabolic model in the last time step.

Table 5 Order of convergence in L^2, H^1 and M -norms for second order parabolic model problem.

Level	$h = k$	$\ u - u_h\ _{H^1}$	Order of convergence	$\ u - u_h\ _{L^2}$	Order of convergence	$\ \kappa - \kappa_h\ _M$	Order of convergence
1	1/2	0.1102		0.0133		0.0397	
2	1/4	0.0493	1.1597	0.0028	2.2400	0.0131	1.5965
3	1/8	0.0224	1.1366	6.70e-04	2.0713	0.0061	1.0977
4	1/16	0.0106	1.0866	1.59e-04	2.0498	0.0029	1.0702
5	1/32	0.0051	1.0483	3.88e-05	2.0344	0.0014	1.0392

problems with an adequate amount of modification. We will include the implementations for the three-dimensional case in our future work.

Acknowledgement

The second author's work is supported by CSIR Extramural Research Grant. The third author announces the support of the Czech Science Foundation (GACR) through the GA23-04766S grant Variational approaches to dynamical problems in continuum mechanics.

References

- [1] Alberty, J., Carstensen, C., Funken, S.A.: Remarks around 50 lines of matlab: short finite element implementation. *Numer. Algorithms* **20**(2-3), 117–137 (1999)
- [2] Bahriawati, C., Carstensen, C.: Three matlab implementations of the lowest-order Raviart-Thomas mfem with a posteriori error control. *Comput. Meth. Appl. Math.* **5**, 333–361 (2005)
- [3] Rahman, T., Valdman, J.: Fast matlab assembly of fem matrices in 2d and 3d: Nodal elements. *Appl. Math. Comput.* **219**(13), 7151–7158 (2013)
- [4] Anjam, I., Valdman, J.: Fast matlab assembly of fem matrices in 2d and 3d: Edge elements. *Appl. Math. Comput.* **267**, 252–263 (2015)
- [5] Funken, S., Praetorius, D., Wissgott, P.: Efficient implementation of adaptive p1-fem in matlab. *Comput. Meth. Appl. Math.* **11**(4), 460–490 (2011)
- [6] Cuvelier, F., Japhet, C., Scarella, G.: An efficient way to assemble finite element matrices in vector languages. *BIT Numer. Math.* **56**, 833–864 (2016)
- [7] Moskovka, A., Valdman, J.: Fast matlab evaluation of nonlinear energies using fem in 2d and 3d: Nodal elements. *Appl. Math. Comput.* **424**, 127048 (2022)
- [8] Raviart, P.A., Thomas, J.M.: Primal hybrid finite element methods for 2nd order elliptic equations. *Math. Comp.* **31**(138), 391–413 (1977)
- [9] Acharya, S.K., Patel, A.: Primal hybrid method for parabolic problems. *Appl. Numer. Math.* **108**, 102–115 (2016)

- [10] Acharya, S.K., Porwal, K.: Primal hybrid finite element method for fourth order parabolic problems. *Appl. Numer. Math.* **152**, 12–28 (2020)
- [11] Wriggers, P., Carstensen, C.: Mixed finite element technologies. CISM Courses and Lectures, Vol. 509, Springer Wien New York, 2009
- [12] Oliari, V.B., Bösing, P.R., Siqueira, D., Devloo, P.R.B.: A posteriori error estimates for primal hybrid finite element methods applied to poisson problem. *J. Comput. Appl. Math.* **441**, 115671 (2024)
- [13] Funken, S., Schmidt, A.: A coarsening algorithm on adaptive red-green-blue refined meshes. *Numer. Algorithms* **87**, 1147–1176 (2021)
- [14] Bey, J.: Simplicial grid refinement: On freudenthal's algorithm and the optimal number of congruence classes. *Numer. Math.* **85**(1), 1–29 (2000)
- [15] Ciarlet, P.G.: The finite element method for elliptic problems. North-Holland, Amsterdam, 1978
- [16] Thomée, V.: Galerkin finite element methods for parabolic problems. Lecture Notes in Mathematics, Springer, Berlin, 1984